Materials Chemistry and Physics 180 (2016) 97–103

Contents lists available at ScienceDirect

Materials Chemistry and Physics

journal homepage: www.elsevier.com/locate/matchemphys

The effect of antimony-tin and indium-tin oxide supports on the catalytic activity of Pt nanoparticles for ammonia electro-oxidation

Júlio César M. Silva [a, b], Ricardo M. Piasentin [b], Estevam V. Spinacé [b], Almir O. Neto [b], Elena A. Baranova [a, *]

[a] Department of Chemical & Biological Engineering, Centre for Catalysis Research and Innovation (CCRI), University of Ottawa, 161 Louis-Pasteur, Ottawa, ON K1N 6N5, Canada

[b] Instituto de Pesquisas Energéticas e Nucleares, IPEN/CNEN-SP, Av. Prof. Lineu Prestes, 2242 Cidade Universitária, CEP 05508-900, São Paulo, SP, Brazil

HIGHLIGHTS

- Oxide support effect on the catalytic activity of Pt towards ammonia electro-oxidation.
- Direct ammonia fuel cell (DAFC) performance using Pt over different supports as anode.
- Pt/C-ITO shows better catalytic activity for ammonia oxidation than Pt/C and Pt/C-ATO.

ARTICLE INFO

Article history:
Received 19 January 2016
Received in revised form
3 May 2016
Accepted 19 May 2016
Available online 2 June 2016

Keywords:
Oxidation
Nanostructures
Chemical synthesis
Electrochemical techniques
Oxides

ABSTRACT

Platinum nanoparticles supported on carbon (Pt/C) and carbon with addition of ITO (Pt/C-ITO $(In_2O_3)_9{\cdot}(SnO_2)_1$) and ATO (Pt/C-ATO $(SnO_2)_9{\cdot}(Sb_2O_5)_1$) oxides were prepared by sodium borohydride reduction method and used for ammonia electro-oxidation reaction (AmER) in alkaline media. The effect of the supports on the catalytic activity of Pt for AmER was investigated using electrochemical (cyclic voltammetry and chronoamperometry) and direct ammonia fuel cell (DAFC) experiments. X-ray diffraction (XRD) showed Pt peaks attributed to the face-centered cubic (fcc) structure, as well as peaks characteristic of In_2O_3 in ITO support and cassiterite SnO_2 phase of ATO support. According to transmission electron micrographs the mean particles sizes of Pt over carbon were 5.4, 4.9 and 4.7 nm for Pt/C, Pt/C-ATO and Pt/C-ITO, respectively. Pt/C-ITO catalysts showed the highest catalytic activity for ammonia electrooxidation in both electrochemical and fuel cell experiments. We attributed this to the presence of In_2O_3 phase in ITO, which provides oxygenated or hydroxide species at lower potentials resulting in the removal of poisonous intermediate, i.e., atomic nitrogen (N_{ads}) and promotion of ammonia electro-oxidation.

© 2016 Elsevier B.V. All rights reserved.

1. Introduction

Ammonia electro-oxidation reaction (AmER) has attracted considerable amount of attention in the recent decade from the standpoint of energy generation in direct ammonia fuel cells (DAFCs), wastewater treatment and ammonia sensor technologies [1–6]. Ammonia has been considered as a potential fuel for alkaline fuel cells because it has low production cost, is easy to handle and to transport as liquid or as concentrated aqueous solution [3,7]. The theoretical charge for ammonia oxidation to N_2 is 4.75 Ah g^{-1} and compares very well with the theoretical charge of 5.02 Ah g^{-1} of methanol in its oxidation to CO_2 [7].

AmER is a slow process at low temperatures (<100 °C) and materials with high catalytic activity are required to improve its kinetics for complete oxidation to nitrogen [5,8,9]. A number of studies have been reported concerning the development of efficient electrocatalysts for ammonia electro-oxidation in alkaline solutions [1,2,4,7–11]. Among them, bulk or nanostructured Pt has been identified as one of the best electrocatalyst for this process, however the issue of poisoning by strongly adsorbed intermediates, like atomic nitrogen, N_{ads} [1,12,13], and Pt cost are two main constrains that have to be overcome before ammonia electro-oxidation technologies can be successfully implemented. Two common strategies

* Corresponding author.
E-mail address: elena.baranova@uottawa.ca (E.A. Baranova).

http://dx.doi.org/10.1016/j.matchemphys.2016.05.047
0254-0584/© 2016 Elsevier B.V. All rights reserved.

include the addition of the second metal to Pt catalyst, i.e., bimetallic Pt-based electrocatalysts [1,5,7,8] and the variation of the catalyst support [1,14,15]. In the former case, the second metal decreases Pt amount and often improves the catalytic activity of Pt via electronic or geometric effect [5,10]. Recently, the use of bimetallic Pt-based electrocatalysts (PtRu/C, PtRh/C, PtAu/C etc.) in direct ammonia fuel cell (DAFC) that operate on NH_4OH in KOH as fuel have been reported [4,5,11,16]. In all cases the addition of the second metal to Pt enhanced the open circuit voltage (OCV) and the power density [5,11,16]. In the latter case, the support can strongly enhance the catalytic activity of Pt either by improving the catalyst dispersion and particle size stabilization or electronic effect, i.e., via metal-support interaction (MSI) also called electronic metal support interaction (EMSI) [17,18]. The MSI usually originates from the charge transfer between the metal and the oxide support [19,20], which in turn affects the activity of the catalytic phase.

Carbon black is a common support for nanosized electrocatalysts in fuel cells, because of its large surface area, high electrical conductivity, porous structures and low cost. However, this inert material does not enhance electrocatalytic activities, but serves mostly as a mechanical support [21–24], because carbon support shows weak MSI and in addition it has low corrosion resistance under fuel cell conditions.

Several oxide supports have been considered for electrocatalytic oxidation of different organic molecules (ethanol, methanol, etc.), among them: SnO_2, $SnO_2{\cdot}SbO_2O_5$ (ATO), $In_2O_3{\cdot}SnO_2$ (ITO), WO_3 and TiO_2 have shown to help the oxidation kinetics [21,25–30]. For instance, indium oxide (In_2O_3) has been used to improve the catalytic performance of methanol and dehydrogenation of ethanol [29,31]. In general, these oxides have high corrosion resistance and their use results in lower decrease in the electrochemical active surface area (ECSA) of the active phase in comparison with carbon support [29,32].

Furthermore, ITO ($In_2O_3{\cdot}SnO_2$) and ATO ($SnO_2{\cdot}Sb_2O_5$) and In_2O_3 have been used as high sensitivity sensors for hydrocarbons, ammonia, CO and H_2 detection. In_2O_3 shows the highest sensitivity to ammonia if compared to ITO and ATO sensors [6], and addition of Pt to In_2O_3 further increases the response for ammonia and other molecules detection [6,33,34]. Recently, Zhong et al. [15] reported results of ammonia electro-oxidation on platinum particles with different morphology that were prepared by electro-deposition on flat ITO substrate. Although authors did not discuss the role of ITO substrate on catalytic activity of Pt, the satisfactory stability of Pt particles was confirmed.

Another support of interest for AmER could be ATO. For instance, Piasentin et al. [35] reported that Pt nanoparticles supported on carbon with 15% of ATO (Pt/C + ATO) showed better catalytic activity than Pt nanoparticles supported on carbon (Pt/C) as anode in a direct ethanol fuel cell (DEFC). This was attributed to the change in the electronic density of Pt (electronic effect) and bifunctional mechanism promoted by ATO oxides.

Therefore, supporting Pt nanoparticles on oxide materials, for instance, ITO and ATO could lead to the improved current densities for AmER and high DAFC power densities. However, despite the above mentioned studies, there are no reports exist that evaluate the role of ITO and ATO oxides on the catalytic activity of Pt nanoparticles and the effect of their addition to carbon support in order to promote ammonia electro-oxidation at lower overpotentials. Hence, aiming at the development of efficient DAFCs, we describe the synthesis of Pt nanoparticles supported on carbon (Pt/C) and on physical mixtures of carbon with ITO (Pt/C-ITO) and ATO (Pt/C-ATO) powders as an anode material in DAFC. First, we show the synthesis of nanostructured Pt catalysts and their characterization by XRD and TEM. Then, we present the electrochemical experiments in the three-electrode electrochemical cell and direct ammonia fuel cell tests.

2. Experimental

Pt/C, Pt/C-ITO and Pt/C-ATO (20 wt% of Pt loading) were prepared by the sodium borohydride reduction process [16,36] using $H_2PtCl_6{\cdot}6H_2O$ (Sigma-Aldrich). For Pt/C-ATO and Pt/C-ITO, a physical mixture of 85 wt% of carbon (Vulcan XC-72) and 15 wt% of ATO powder ($(SnO_2)_9{\cdot}(Sb_2O_5)_1$) (Sigma-Aldrich) and 85 wt% of carbon (Vulcan XC72) and 15 wt% of ITO powder ($(In_2O_3)_9{\cdot}(SnO_2)_1$) (Sigma-Aldrich), respectively was used as a support. The particle size of ITO and ATO is ~50 nm and their specific surface area (a_s) is 27 $m^2\ g^{-1}$ and 47 $m^2\ g^{-1}$, respectively if compared to the particle size of 50 nm and $a_s = 239\ m^2\ g^{-1}$ for carbon (Vulcan XC-72) [37]. In the synthesis process the support materials were first dispersed in an isopropyl alcohol/water solution (50/50, v/v) and homogenized under stirring to form a uniform mixture of carbon and oxides. Then the metal precursor was added and placed in an ultrasonic bath for 5 min. After that, a solution of $NaBH_4$ in 0.1 M KOH was added in one portion under stirring at room temperature and the resulting solution was kept under stirring for 15 min more. After this, the final mixture was filtered and the solids washed with water and then dried at 70 °C for 2 h. The commercial electrocatalyst Pt/C BASF was used in order to compare the obtained results from ammonia electro-oxidation.

The electrocatalysts were characterized by X-ray diffraction (XRD) using a Rigaku diffractometer model Miniflex II using Cu Kα radiation source (0.15406 nm). The X-ray diffraction patterns were recorded in the range of $2\theta = 20°–90°$ with a step size of 0.05° and a scan time of 2 s per step.

Transmission electron microscopy (TEM) analysis were carried out using a JEOL transmission electron microscope model JEM-2100 operated at 200 kV in order to obtain the morphology, distribution and nanoparticles size which were determined by counting about 200 particles at different regions of the materials.

Electrochemical measurements were carried out using a potentiostat/galvanostat PGSTAT 30 Autolab and a conventional three-electrode electrochemical cell at room temperature, unless otherwise stated. A platinum mesh and an Ag/AgCl (KCl 3 M) were used as the counter and reference electrodes, respectively. Glassy carbon (GC) electrode (0.166 cm^2 of geometric area) was used to support the nanostructured Pt electrocatalysts. Before each experiment, the GC support was polished with alumina suspension (1 μm) and washed in deionized water. Ultrapure deionized water obtained from a Milli-Q system (Millipore®) was used in all experimental procedures.

The working electrode was constructed by dispersing 8 mg of the electrocatalyst powder in 1 mL water and mixing for 15 min in an ultrasonic bath. Shortly thereafter, 20 μL of 5% Nafion® solution was added to the suspension, which was mixed again for 20 min in an ultrasonic bath. Aliquots of 16 μL of the dispersion fluid were placed onto the GC surface. Finally, the electrode was dried at 60 °C for 20 min. All the electrochemical measurements were performed in a 1 M KOH solution with and without ammonia.

Cyclic voltammograms (CV) were carried out at a scan rate of 20 mV s^{-1} between − 0.85 V and 0.0 V *vs* Ag/AgCl. The electrocatalysts were cycled for ten consecutive cycles in ammonia free solutions and three consecutive cycles in ammonia containing solutions. Chronoamperometric experiments were carried out for 1800 s at −0.35 V *vs* Ag/AgCl. The electro-oxidation of ammonia was performed in a 1 M (KOH + NH_4OH) solution. All potentials are reported against Ag/AgCl reference electrode, unless otherwise stated.

The catalyst electrochemical active surface area (ECSA) was measured using the charge involved in the hydrogen desorption

region between −0.84 and −0.57 V in 1 M KOH. The ammonia oxidation current in CV and CA experiments is normalized per ECSA to compare the intrinsic activity of the supported electrocatalysts, unless otherwise stated.

DAFCs experiments were conducted as already described elsewhere [4,5,11,16]. In these experiments a single cell set at 50 °C with an electrode area of 5 cm^2 was employed. The temperature of the oxygen humidifier was maintained at 85 °C. All electrodes were constructed with Pt loading of 2 mg cm^{-2} on both anode and cathode. For all experiments, a commercial Pt/C (BASF) was used as cathode. A Nafion® 117 membrane previously exposed to 6 M KOH for 24 h [16,38] was used for fuel cell experiments.

3. Results and discussion

Fig. 1 shows the XRD patterns of the Pt/C BASF, Pt/C, Pt/C-ITO and Pt/C-ATO. In all XRD patterns, a broad peak at about 25 °2θ is due to the (022) reflection of the hexagonal structure of Vulcan XC 72 carbon [11,16]. The face-centered cubic structure (fcc) of Pt is confirmed by the diffraction peaks at approximately 2θ = 39°, 46°, 67° and 81° that correspond to (111), (200), (220) and (311) crystal planes, respectively [11,16]. For Pt/C-ITO electrocatalyst, peaks characteristic of Pt fcc structure and peaks at about 2θ = 31°, 36°, 51°, 60°, corresponding to In_2O_3 cubic structure are also seen [29,39]. The pattern of Pt/C-ATO, besides the Pt (fcc) phase also shows diffraction peaks at around 2θ = 27°, 34°, 38°, 52°, 55°, 62°, 65° and 66°, which are characteristic of cassiterite SnO_2 phase

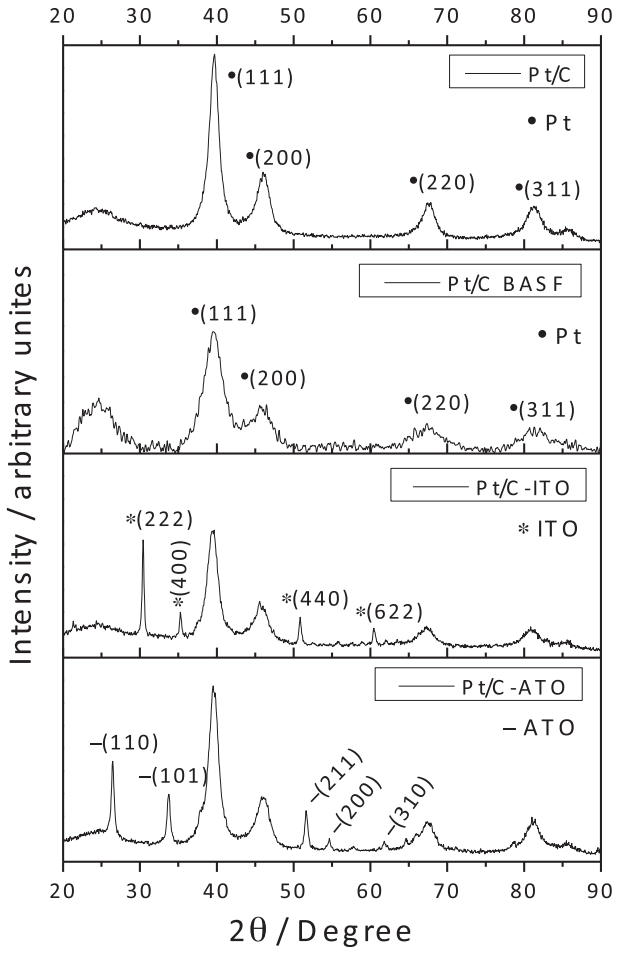

Fig. 1. X-ray diffraction patterns of the Pt/C, Pt/C BASF, Pt/C-ITO and Pt/C-ATO catalysts.

[40,41]. The crystallite size, estimated using Scherrer equation and (220) peak [8,42] are 2.9 nm for Pt/C BASF, 5.1 nm for Pt/C, 4.3 nm for Pt/C-ATO and 3.9 nm for Pt/C-ITO.

Fig. 2 shows TEM micrographs and histograms of the particle mean diameter distribution for Pt/C, Pt/C-ITO and Pt/C-ATO. In all cases the nanoparticles were well dispersed on the carbon support. On Pt/C-ITO and Pt/C-ATO there are some regions that are rich in ITO and ATO [40,43], as can be seen in the insert in macrographs 2b and 2c. The nanoparticles over these supports are more agglomerated that on carbon. In order to estimate the nanoparticles mean diameter about 300 particles supported on carbon were measured, the obtained values were 5.4 ± 1.7 nm for Pt/C, 4.9 ± 1.6 nm for Pt/C-ATO and 4.7 ± 1.3 nm for Pt/C-ITO. These values are in a good agreement with the crystallite sizes obtained using Scherrer equation [44]. The Pt/C-ITO and Pt/C-ATO nanoparticles average sizes are slightly smaller than Pt/C nanoparticles, this is related to the MSI effect, where the addition of ITO and ATO during the synthesis prevents nanoparticle growth and agglomeration. It has been reported earlier [19,20], that oxide supports promote nanoparticles stabilization through MSI. For instance, Zhang et al. [45] showed that Pt nanoparticles supported on the mixture of SnO_2 and carbon resulted in smaller particle size than for Pt supported on carbon only. XPS analysis of Pt4f peak showed that the Pt(0) binding energy shifted negatively, confirming the electron transfer from Sn to Pt in the Pt/SnO_2/C catalyst. Similar, MSI of the electronic type was observed for Pt/ITO [43] and for Pt nanoparticles deposited on various oxides: TiO_2, CeO_2, MoO_2, WO_2, SnO_2, $SrRuO_3$ and RuO_2 [46]

Fig. 3 shows the cyclic voltammetry of Pt nanoparticles deposited on various supports in 1 M KOH. For Pt/C and Pt/C BASF, the hydrogen adsorption/desorption region is well defined between −0.8 V to −0.6 V [5,11]. The ECSA estimated by hydrogen desorption were 27 $m^2\ g_{Pt}^{-1}$, 30 $m^2\ g_{Pt}^{-1}$, 22 $m^2\ g_{Pt}^{-1}$ and 20 $m^2\ g_{Pt}^{-1}$, to Pt/C, Pt/C BASF, Pt/C-ATO and Pt/C-ITO, respectively. These results are in agreement with the reported values [47,48]. The potential region from −0.30 to 0.0 V is associated with the formation of an oxide layer on the platinum surface [5,49] and the cathodic peak at around −0.25 V is due to platinum oxide reduction [5,50]. For Pt/C-ITO and Pt/C-ATO electrocatalysts, the hydrogen region has the same characteristic shape typical for Pt electrode. The peak current for PtO_x formation (~−0.3 V) is the highest for Pt/C-ITO following by Pt/C-ATO and Pt/C. The same order of current magnitude is preserved in the cathodic scan during PtO_x reduction (~−0.25 V). For both Pt/C-ITO and Pt/C-ATO, the reduction peak is shifted to lower potentials compared to Pt/C, indicating that this process is less thermodynamically favorable on oxide supports. Similar behavior was observed in the literature for Pt supported on different oxide materials [51,52] and was associated with the amount of oxides formed during the anodic scan [53].

The cyclic voltammetry of Pt electrocatalysts in 1 M (KOH + NH_4OH) are shown in Fig. 4. It can be seen that Pt/C-ITO has the lowest onset potential following by Pt/C-ATO, Pt/C BASF and then Pt/C. Furthermore, Pt/C-ITO shows the highest peak current density for ammonia electrooxidation than for Pt/C-ATO and Pt/C, indicating that using C + ITO and C + ATO as a support improves the catalytic activity for ammonia electro-oxidation compared with carbon. This can be attributed to the presence of In_2O_3 and SnO_2 oxides in ITO and ATO supports. The best performance obtained using Pt/C-ITO, might be attributed to In_2O_3 phase, since ITO used in our experiments consists of 90% of In_2O_3 and 10% of SnO_2. Enhancement of catalytic activity was also observed earlier on Pt/C + ITO for ethanol electro-oxidation [29]. The activity of Pt/C-ATO was higher than Pt/C, but was inferior to Pt/C-ITO. This could be related to the high amount of SnO_2 (90% of SnO_2 and 10% of SbO_2O_5) in ATO and its lower conductivity compared to ITO as will be

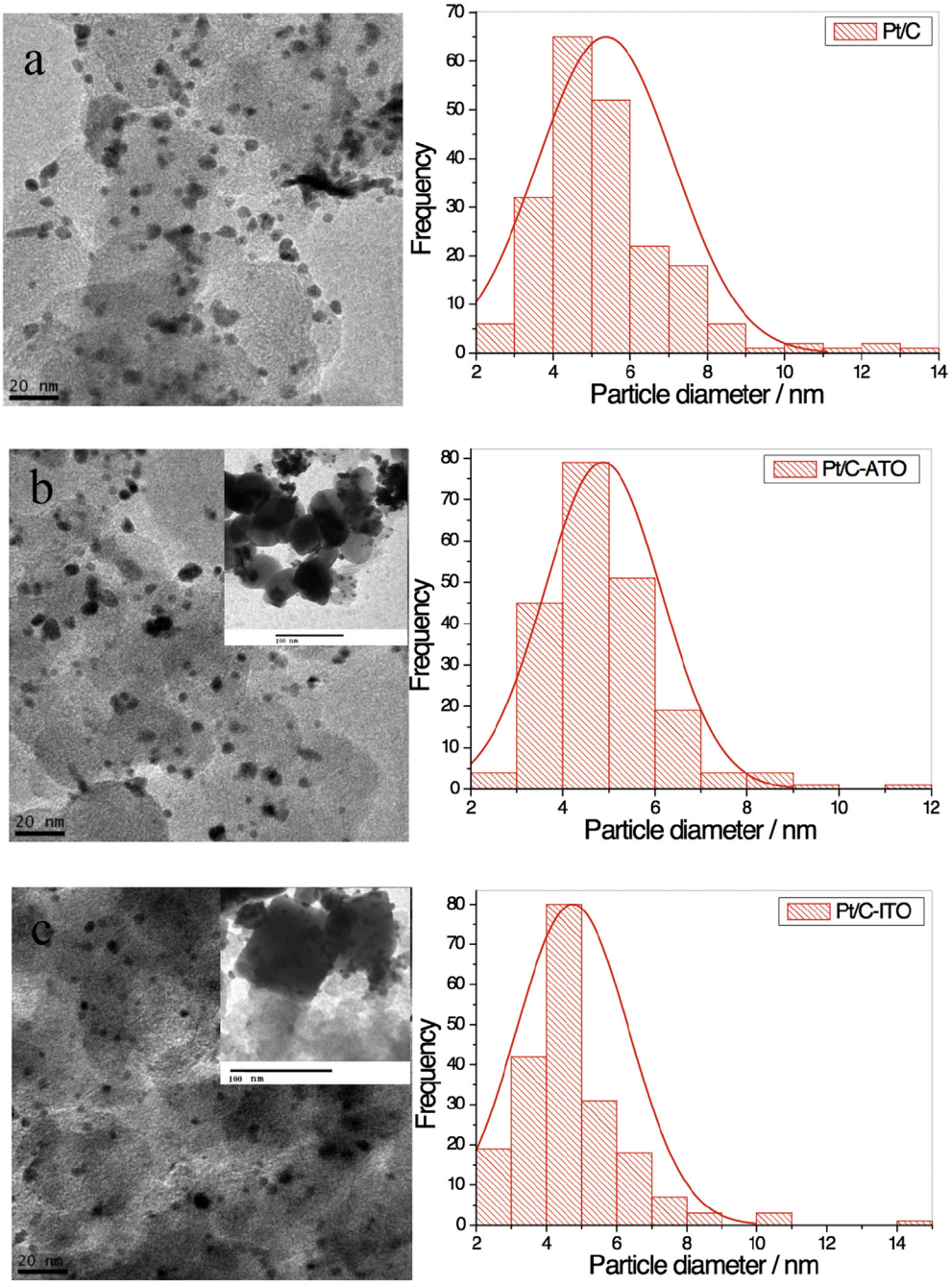

Fig. 2. The TEM micrographs and histograms of (a) Pt/C, (b) Pt/C-ATO and (c) Pt/C-ITO electrocatalysts. Insert in (a) the region rich in ATO and in (b) the region rich in ITO.

discussed later.

The onset potential for AmER on Pt/C-ITO is comparable or lower than those reported in the literature [1,5,7], however very often it is difficult to directly compare the obtained current densities with the literature due to the different parameters adopted by the authors. Some authors normalize oxidation current by platinum loading [11], some by total metal loading [5], some by geometric area of the electrode [1], and others by the ECSA found from the charge involved in the hydrogen desorption region [7]. Additionally, the electrochemical experiments are often conducted in different ammonia concentration using different reference electrodes [1,5,7,10,11]. For instance, Vidal-Iglesias et al. [7] reported their results related to ammonia electro-oxidation on polycrystalline platinum nanoparticles normalized by ECSA evaluated from the charge involved in the hydrogen desorption region. The reported peak current density of ammonia electro-oxidation on Pt nanoparticles [7] is lower than that reported in the present study. However, they used lower ammonia concentration (0.2 M) and unsupported Pt nanoparticles.

Comparison of the Pt/C catalyst synthesized in the present work and the commercial Pt/C BASF reveals similar behavior of the two catalysts with somewhat lower onset potential and lower peak current density for Pt/C BASF (Fig. 4, curves a and d) This differences may be related to the particle size since the mean crystallite size of Pt/C BASF is smaller than the synthesized Pt/C catalyst.

Fig. 5 shows the chronoamperometry curves at − 0.35 V in the

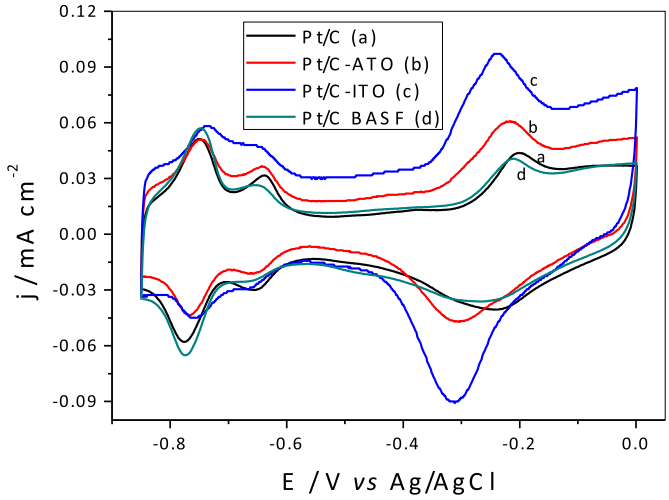

Fig. 3. Cyclic voltammograms of Pt/C, Pt/C BASF, Pt/C-ATO and Pt/C-ITO electrocatalysts in 1 M KOH at $\nu = 20$ mV s^{-1}.

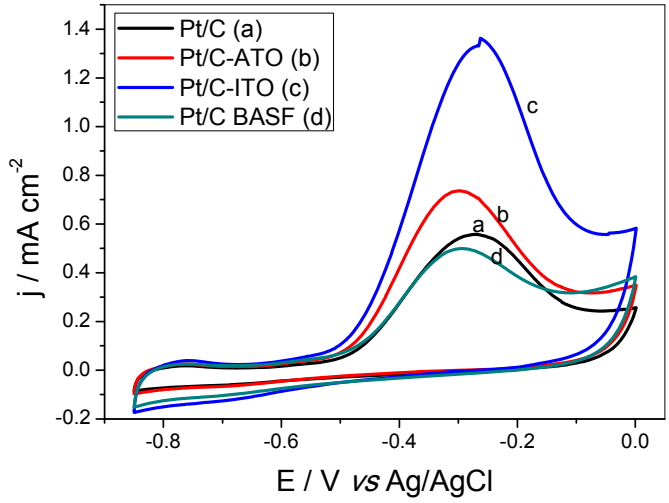

Fig. 4. Cyclic voltammograms of Pt/C, Pt/C-ATO, Pt/C-ITO and Pt/C BASF electrocatalysts in 1 M (KOH + NH_4OH) at $\nu = 20$ mV s^{-1}.

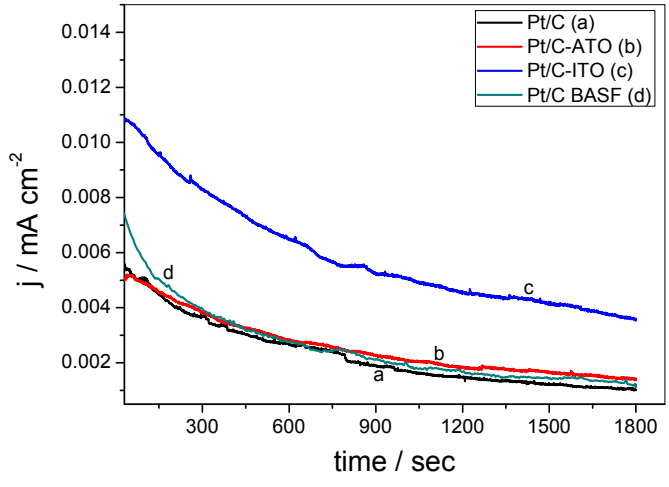

Fig. 5. Chronoamperometric measurements at −0.35 V *vs* Ag/AgCl, on Pt/C, Pt/C BASF, Pt/C-ATO and Pt/C-ITO electrocatalysts in 1 M (KOH + NH_4OH).

ammonia containing solution. Similar to CV experiments, Pt/C-ITO has the highest current density compared to other electrocatalysts, whereas the current density on Pt/C was the lowest. For all four catalysts the current density decreases with time and does not reach the steady-state after half an hour, which indicates that the catalyst surface deactivates with time. According to the mechanism of AmER in alkaline media proposed by Gerischer and Mauerer [12], the deactivation is due to the formation of the strongly adsorbed atomic nitrogen, N_{ads}. As was reported earlier [54], AmER on metal oxides may result in OH_{ads} (MO_nOH_{ads}) and formation of hidroxylamine (NH_2OH), which is subsequently converted to products such as nitrite and nitrate. Thus the presence of hydrohydes allows the reaction to proceed through the passway that decreases or eliminates N_{ads} formation. In this context, the ITO and ATO supports could provide oxygenated species, which influence the adsorption properties of Pt, i.e., weaken N_{ads} bond strength and/or modify the reaction pathway. This is supported by the literature reports, where it is illustrated that ITO and ATO provide oxygenated species at lower potentials, which contribute to the oxidation of intermediates products from different molecules in electrochemical process [21,29,40,41]. Thus, it is proposed that the presence of oxide supports enhances ammonia oxidation kinetics by decreasing the amount of N_{ads} species on Pt nanoparticles. Donley et al. [55] reported that ITO presents high concentration of hydroxide and oxihydroxide species on the surface, this aspect might be responsible for the highest catalytic activity of Pt/C-ITO. An evidence of the synergic effect that affects the intrinsic catalytic activity of Pt rather than geometric effect, i.e., smaller nanoparticle size, is further confirmed by ECSA values. The material with the lowest ECSA, Pt/C-ITO, showed the highest catalytic activity for AmER. The interaction between platinum nanoparticles and the oxide support can result in charge redistribution due to the electronic MSI effect, which may decrease the adsorption energy of intermediates at the catalyst surface [19,20].

Another factor that needs to be addressed is the size of nanoparticles. It has been reported that platinum nanoparticles smaller than 5 nm shows stronger adsorption of H^+ and OH^- species [56]. However, the interaction of OH^- is more enhanced as the nanoparticles get smaller than the interaction of H^+ [56,57]. In this sense, as the interaction of the Pt-OH increases, it decreases the interaction of N_{ads} with the platinum. This could explain the slightly higher current density obtained with Pt/C BASF than Pt/C in the CA experiments.

Fig. 6 shows the polarization and power density curves for a DAFC using Pt/C, Pt/C-ITO and Pt/C-ATO catalysts at the anode and 1 M (KOH + NH_4OH) electrolyte at 50 °C. As in CV and CA experiments, the highest performance of DAFC is reached with Pt/C-ITO anode than with Pt/C-ATO and Pt/C electrocatalysts. Using Pt/C-ITO the open circuit voltage was higher (0.50 V) than for Pt/C (0.48 V) and Pt/C-ATO (0.47 V). The results for Pt/C are in agreement with the previous literature reports [5,11,16]. The recent work [16] reports DAFC results using the commercial Pt/C BASF catalyst, as can be seen the results obtained using the commercial material is similar to the results found using Pt/C prepared in the present study. The maximum DAFC power density was 2.9, 2.4 and 3.3 mW cm^{-2} for Pt/C, Pt/C-ATO and Pt/C-ITO, respectively. Therefore, addition of ITO improves the DAFC power density if compared to carbon support only. In the recent study Okanishi et al. showed that addition of SnO_2 phase to Pt (C-Pt/SnO_2) activated the dehydrogenation of ammonia and this anode materials outperformed Pt/C in an ammonia-fueled anion exchange membrane fuel cells [51].

Furthermore, the best performance of C-ITO support compared to C-ATO supports could be related to the higher conductivity of ITO than ATO [39,58]. The conductivity of ATO varies from 0.09 to

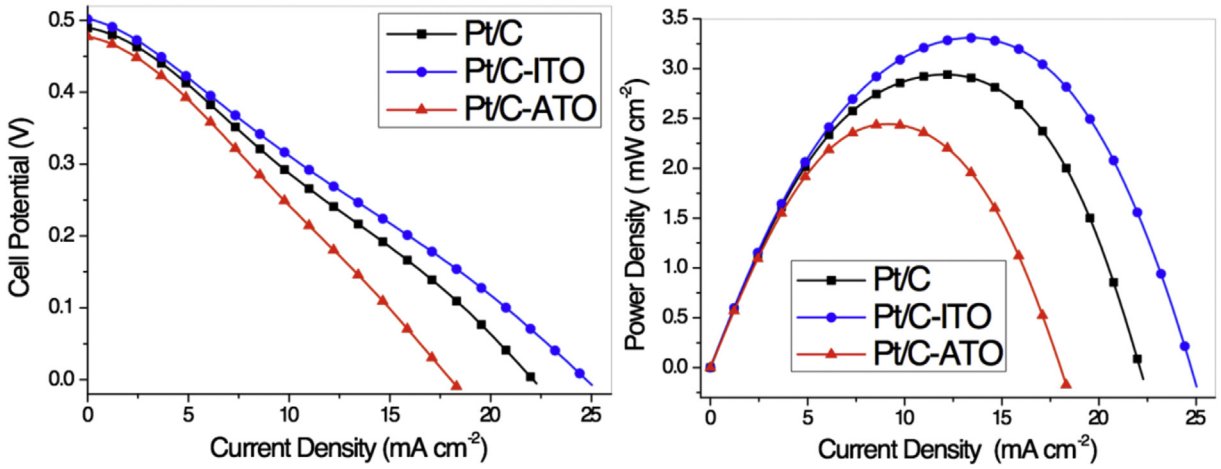

Fig. 6. Polarization (left) and power density (right) curves of a 5 cm^2 DAFC at 50 °C, using 1 M (KOH + NH_4OH).

0.83 S cm^{-1} depending on antimony amount between 3 and 11% in SnO_2 [21], whereas the reported conductivity of ITO is up to 1000 S cm^{-1} [39,59]. All in all, the interaction between Pt and In_2O_3, which contains both oxygenized species and In atoms on the surface [60], improves the ammonia electro-oxidation reaction.

4. Conclusions

In the present work we show that addition of ITO oxide to carbon support for Pt nanoparticles (Pt/C-ITO) significantly improves the ammonia electro-oxidation. As we found by TEM, the platinum nanoparticles were well dispersed on the carbon support, however showed slightly larger particle size and more agglomeration compared to Pt supported on C-ATO and C-ITO support. The lowest onset potential and the highest peak current density for ammonia electro-oxidation in CV experiments were obtained using Pt/C-ITO. In CA experiments, the current density of ammonia electro-oxidation on Pt/C-ITO was about 2.5 times, 2.8 times and 3.3 times higher than that obtained on Pt/C-ATO, commercial Pt/C BASF and Pt/C, respectively. Using Pt/C-ITO as an anode in DAFC at 50 °C the maximum power density was 37% and 14% higher than those obtained using Pt/C-ATO and Pt/C, respectively. We propose that ITO support with the higher conductivity than ATO, provides oxygenated species at lower potentials resulting in the weakening of the adsorption strength of poisonous N_{ads} intermediate and/or modification of the reaction pathway through hydrohylamine (NH_2OH) formation thus preventing the Pt surface from deactivation in DAFCs.

Acknowledgements

The authors wish to thank FAPESP process numbers (2013/01577-0, 2014/09868-6) and CNPq for the financial support, Dr. Cristiane Agelica Ottoni and laboratório de microscopia do centro de ciências e tecnologia de materiais (CCTM) for TEM measurements.

References

[1] B.K. Boggs, G.G. Botte, Optimization of Pt–Ir on carbon fiber paper for the electro-oxidation of ammonia in alkaline media, Electrochim. Acta 55 (2010) 5287–5293.
[2] A. Allagui, S. Sarfraz, E.A. Baranova, NixPd1−x (x = 0.98, 0.93, and 0.58) nanostructured catalysts for ammonia electrooxidation in alkaline media, Electrochim. Acta 110 (2013) 253–259.
[3] S. Suzuki, H. Muroyama, T. Matsui, K. Eguchi, Fundamental studies on direct ammonia fuel cell employing anion exchange membrane, J. Power Sources 208 (2012) 257–262.
[4] M.H.M.T. Assumpção, S.G. da Silva, R.F.B. De Souza, G.S. Buzzo, E.V. Spinacé, M.C. Santos, A.O. Neto, J.C.M. Silva, Investigation of PdIr/C electrocatalysts as anode on the performance of direct ammonia fuel cell, J. Power Sources 268 (2014) 129–136.
[5] M.H.M.T. Assumpção, R.M. Piasentin, P. Hammer, R.F.B. De Souza, G.S. Buzzo, M.C. Santos, E.V. Spinacé, A.O. Neto, J.C.M. Silva, Oxidation of ammonia using PtRh/C electrocatalysts: fuel cell and electrochemical evaluation, Appl. Catal. B Environ. 174–175 (2015) 136–144.
[6] V. Romanovskaya, M. Ivanovskaya, P. Bogdanov, A study of sensing properties of Pt- and Au-loaded In2O3 ceramics, Sensors Actuators B Chem. 56 (1999) 31–36.
[7] F.J. Vidal-Iglesias, J. Solla-Gullón, V. Montiel, J.M. Feliu, A. Aldaz, Screening of electrocatalysts for direct ammonia fuel cell: ammonia oxidation on PtMe (Me: Ir, Rh, Pd, Ru) and preferentially oriented Pt(1 0 0) nanoparticles, J. Power Sources 171 (2007) 448–456.
[8] T.L. Lomocso, E.A. Baranova, Electrochemical oxidation of ammonia on carbon-supported bi-metallic PtM (M = Ir, Pd, SnOx) nanoparticles, Electrochim. Acta 56 (2011) 8551–8558.
[9] L.A. Diaz, A. Valenzuela-Muñiz, M. Muthuvel, G.G. Botte, Analysis of ammonia electro-oxidation kinetics using a rotating disk electrode, Electrochim. Acta 89 (2013) 413–421.
[10] A. Allagui, M. Oudah, X. Tuaev, S. Ntais, F. Almomani, E.A. Baranova, Ammonia electro-oxidation on alloyed PtIr nanoparticles of well-defined size, Int. J. Hydrogen Energy 38 (2013) 2455–2463.
[11] J.C.M. Silva, S.G. da Silva, R.F.B. De Souza, G.S. Buzzo, E.V. Spinacé, A.O. Neto, M.H.M.T. Assumpção, PtAu/C electrocatalysts as anodes for direct ammonia fuel cell, Appl. Catal. A General 490 (2015) 133–138.
[12] H. Gerischer, A. Mauerer, Untersuchungen Zur anodischen Oxidation von Ammoniak an Platin-Elektroden, J. Electroanal. Chem. Interfacial Electrochem. 25 (1970) 421–433.
[13] A.C.A. de Vooys, M.T.M. Koper, R.A. van Santen, J.A.R. van Veen, The role of adsorbates in the electrochemical oxidation of ammonia on noble and transition metal electrodes, J. Electroanal. Chem. 506 (2001) 127–137.
[14] J. Liu, B. Liu, Z. Ni, Y. Deng, C. Zhong, W. Hu, Improved catalytic performance of Pt/TiO2 nanotubes electrode for ammonia oxidation under UV-light illumination, Electrochim. Acta 150 (2014) 146–150.
[15] J. Liu, C. Zhong, Y. Yang, Y.T. Wu, A.K. Jiang, Y.D. Deng, Z. Zhang, W.B. Hu, Electrochemical preparation and characterization of Pt particles on ITO substrate: morphological effect on ammonia oxidation, Int. J. Hydrogen Energy 37 (2012) 8981–8987.
[16] M.H.M.T. Assumpção, S.G. da Silva, R.F.B. de Souza, G.S. Buzzo, E.V. Spinacé, A.O. Neto, J.C.M. Silva, Direct ammonia fuel cell performance using PtIr/C as anode electrocatalysts, Int. J. Hydrogen Energy 39 (2014) 5148–5152.
[17] D. de Caro, J.S. Bradley, Surface spectroscopic study of carbon monoxide adsorption on nanoscale nickel colloids prepared from a zerovalent organometallic precursor, Langmuir 13 (1997) 3067–3069.
[18] R. Imbihl, in: Andrzej Wieckowski, Elena R. Savinova, Constantinos G. Vayenas (Eds.), Catalysis and Electrocatalysis at Nanoparticle Surfaces, vol. 44, Angewandte Chemie International Edition, 2005, 359–359.
[19] Q. Fu, T. Wagner, Interaction of nanostructured metal overlayers with oxide surfaces, Surf. Sci. Rep. 62 (2007) 431–498.
[20] R.J. Isaifan, E.A. Baranova, Effect of ionically conductive supports on the catalytic activity of platinum and ruthenium nanoparticles for ethylene complete oxidation, Catal. Today 241 (Part A) (2015) 107–113.
[21] K.-S. Lee, I.-S. Park, Y.-H. Cho, D.-S. Jung, N. Jung, H.-Y. Park, Y.-E. Sung, Electrocatalytic activity and stability of Pt supported on Sb-doped SnO2

nanoparticles for direct alcohol fuel cells, J. Catal. 258 (2008) 143–152.
[22] K.-Y. Chan, J. Ding, J. Ren, S. Cheng, K.Y. Tsang, Supported mixed metal nanoparticles as electrocatalysts in low temperature fuel cells, J. Mater. Chem. 14 (2004) 505–516.
[23] K.-W. Park, Y.-E. Sung, S. Han, Y. Yun, T. Hyeon, Origin of the enhanced catalytic activity of carbon nanocoil-supported PtRu alloy electrocatalysts, J. Phys. Chem. B 108 (2003) 939–944.
[24] I.-S. Park, K.-W. Park, J.-H. Choi, C.R. Park, Y.-E. Sung, Electrocatalytic enhancement of methanol oxidation by graphite nanofibers with a high loading of PtRu alloy nanoparticles, Carbon 45 (2007) 28–33.
[25] A.C.C. Tseung, K.Y. Chen, Hydrogen spill-over effect on Pt/WO3 anode catalysts, Catal. Today 38 (1997) 439–443.
[26] J. Nandenha, R.F.B. Souza, M.H.M.T. Assumpção, E.V. Spinacé, A.O. Neto, Preparation of PdAu/C-Sb2O5·SnO2 electrocatalysts by borohydride reduction process for direct formic acid fuel cell, Ionics (2013) 1–7.
[27] J.C. Castro, R.M. Antoniassi, R.R. Dias, M. Linardi, E.V. Spinacé, A.O. Neto, Preparation of PtSnRh/C-Sb 2O 5·SnO 2 electrocatalysts by an alcohol reduction process for direct ethanol fuel cell, Ionics 18 (2012) 781–786.
[28] A.L. Santos, D. Profeti, P. Olivi, Electrooxidation of methanol on Pt microparticles dispersed on SnO2 thin films, Electrochim. Acta 50 (2005) 2615–2621.
[29] R.S. Henrique, R.F.B. De Souza, J.C.M. Silva, J.M.S. Ayoub, R.M. Piasentin, M. Linardi, E.V. Spinace, M.C. Santos, A.O. Neto, Preparation of Pt/C-In2O3 center dot SnO2 electrocatalysts by borohydride reduction process for ethanol electro-oxidation, Int. J. Electrochem. Sci. 7 (2012) 2036–2046.
[30] H. Hua, C. Hu, Z. Zhao, H. Liu, X. Xie, Y. Xi, Pt nanoparticles supported on submicrometer-sized TiO2 spheres for effective methanol and ethanol oxidation, Electrochim. Acta 105 (2013) 130–136.
[31] N. Iwasa, T. Mayanagi, N. Ogawa, K. Sakata, N. Takezawa, New catalytic functions of Pd–Zn, Pd–Ga, Pd–In, Pt–Zn, Pt–Ga and Pt–In alloys in the conversions of methanol, Catal. Lett. 54 (1998) 119–123.
[32] J. Parrondo, F. Mijangos, B. Rambabu, Platinum/tin oxide/carbon cathode catalyst for high temperature PEM fuel cell, J. Power Sources 195 (2010) 3977–3983.
[33] Y. Wang, B. Liu, D. Cai, H. Li, Y. Liu, D. Wang, L. Wang, Q. Li, T. Wang, Room-temperature hydrogen sensor based on grain-boundary controlled Pt decorated In2O3 nanocubes, Sensors Actuators B Chem. 201 (2014) 351–359.
[34] Y.-S. Shim, H.G. Moon, D.H. Kim, H.W. Jang, C.-Y. Kang, Y.S. Yoon, S.-J. Yoon, Transparent conducting oxide electrodes for novel metal oxide gas sensors, Sensors Actuators B Chem. 160 (2011) 357–363.
[35] R.M. Piasentin, E.V. Spinace, M.M. Tusi, A.O. Neto, Preparation of PdPtSn/C-Sb(2)O(5 center dot)SnO(2) electrocatalysts by borohydride reduction for ethanol electro-oxidation in alkaline medium, Int. J. Electrochem. Sci. 6 (2011) 2255–2263.
[36] A.O. Neto, S.G. da Silva, G.S. Buzzo, R.F.B. de Souza, M.H.M.T. Assumpção, E.V. Spinacé, J.C.M. Silva, Ethanol electrooxidation on PdIr/C electrocatalysts in alkaline media: electrochemical and fuel cell studies, Ionics 21 (2015) 487–495.
[37] V.T. Thanh Ho, K.C. Pillai, H.-L. Chou, C.-J. Pan, J. Rick, W.-N. Su, B.-J. Hwang, J.-F. Lee, H.-S. Sheu, W.-T. Chuang, Robust non-carbon Ti0.7Ru0.3O2 support with co-catalytic functionality for Pt: enhances catalytic activity and durability for fuel cells, Energy & Environ. Sci. 4 (2011) 4194–4200.
[38] H. Hou, S. Wang, W. Jin, Q. Jiang, L. Sun, L. Jiang, G. Sun, KOH modified Nafion112 membrane for high performance alkaline direct ethanol fuel cell, Int. J. Hydrogen Energy 36 (2011) 5104–5109.
[39] W.-L. Qu, D.-M. Gu, Z.-B. Wang, J.-J. Zhang, High stability and high activity Pd/ITO-CNTs electrocatalyst for direct formic acid fuel cell, Electrochim. Acta 137 (2014) 676–684.
[40] A. Oliveira Neto, M. Brandalise, R.R. Dias, J.M.S. Ayoub, A.C. Silva, J.C. Penteado, M. Linardi, E.V. Spinacé, The performance of Pt nanoparticles supported on Sb2O5.SnO2, on carbon and on physical mixtures of Sb2O5.SnO2 and carbon for ethanol electro-oxidation, Int. J. Hydrogen Energy 35 (2010) 9177–9181.
[41] J.M.S. Ayoub, R.F.B. De Souza, J.C.M. Silva, R.M. Piasentin, E.V. Spinace, M.C. Santos, A.O. Neto, Ethanol electro-oxidation on PtSn/C-ATO electrocatalysts, Int. J. Electrochem. Sci. 7 (2012) 11351–11362.
[42] J.C.M. Silva, B. Anea, R.F.B. De Souza, M.H.M.T. Assumpcao, M.L. Calegaro, A.O. Neto, M.C. Santos, Ethanol oxidation reaction on IrPtSn/C electrocatalysts with low Pt content, J. Braz. Chem. Soc. 24 (2013) 1553–1560.
[43] S. Zhao, A.E. Wangstrom, Y. Liu, W.A. Rigdon, W.E. Mustain, Stability and activity of Pt/ITO electrocatalyst for oxygen reduction reaction in alkaline media, Electrochim. Acta 157 (2015) 175–182.
[44] Y. Guan, M. Dai, T. Liu, Y. Liu, F. Liu, X. Liang, H. Suo, P. Sun, G. Lu, Effect of the dispersants on the performance of fuel cell type CO sensor with Pt–C/Nafion electrodes, Sensors Actuators B Chem. 230 (2016) 61–69.
[45] N. Zhang, S. Zhang, C. Du, Z. Wang, Y. Shao, F. Kong, Y. Lin, G. Yin, Pt/Tin oxide/carbon nanocomposites as promising oxygen reduction electrocatalyst with improved stability and activity, Electrochim. Acta 117 (2014) 413–419.
[46] M.E. Scofield, C. Koenigsmann, D. Bobb-Semple, J. Tao, X. Tong, L. Wang, C.S. Lewis, M.B. Vukmirovic, Y. Zhu, R.R. Adzic, S.S. Wong, Correlating the chemical composition and size of various metal oxide substrates with the catalytic activity and stability of as-deposited Pt nanoparticles for the methanol oxidation reaction, Catal. Sci. Technol. 6 (2016) 2435–2450.
[47] A.M. Chaparro, A.J. Martín, M.A. Folgado, B. Gallardo, L. Daza, Comparative analysis of the electroactive area of Pt/C PEMFC electrodes in liquid and solid polymer contact by underpotential hydrogen adsorption/desorption, Int. J. Hydrogen Energy 34 (2009) 4838–4846.
[48] J.F.M.W.F.S.P.E.S.K.D.B.J. Chastain, Handbook of XRay Photoelectron Spectroscopy: a Reference Book of Standard Spectra for Identification and Interpretation of XPS, Data, Perkin-Elmer, Physical Electronics Division, 1992.
[49] L. Jiang, A. Hsu, D. Chu, R. Chen, Ethanol electro-oxidation on Pt/C and PtSn/C catalysts in alkaline and acid solutions, Int. J. Hydrogen Energy 35 (2010) 365–372.
[50] L. Ma, D. Chu, R. Chen, Comparison of ethanol electro-oxidation on Pt/C and Pd/C catalysts in alkaline media, Int. J. Hydrogen Energy 37 (2012) 11185–11194.
[51] R. Crisafulli, R.M. Antoniassi, A. Oliveira Neto, E.V. Spinacé, Acid-treated PtSn/C and PtSnCu/C electrocatalysts for ethanol electro-oxidation, Int. J. Hydrogen Energy 39 (2014) 5671–5677.
[52] A.O. Neto, M.M. Tusi, N.S. de Oliveira Polanco, S.G. da Silva, M. Coelho dos Santos, E.V. Spinacé, PdBi/C electrocatalysts for ethanol electro-oxidation in alkaline medium, Int. J. Hydrogen Energy 36 (2011) 10522–10526.
[53] E.E. Switzer, T.S. Olson, A.K. Datye, P. Atanassov, M.R. Hibbs, C.J. Cornelius, Templated Pt-Sn electrocatalysts for ethanol, methanol and CO oxidation in alkaline media, Electrochim. Acta 54 (2009) 989–995.
[54] N.J. Bunce, D. Bejan, Mechanism of electrochemical oxidation of ammonia, Electrochim. Acta 56 (2011) 8085–8093.
[55] C. Donley, D. Dunphy, D. Paine, C. Carter, K. Nebesny, P. Lee, D. Alloway, N.R. Armstrong, Characterization of indium-tin oxide interfaces using X-ray photoelectron spectroscopy and redox processes of a chemisorbed probe molecule: effect of surface pretreatment conditions, Langmuir 18 (2002) 450–457.
[56] J. Perez, V.A. Paganin, E. Antolini, Particle size effect for ethanol electro-oxidation on Pt/C catalysts in half-cell and in a single direct ethanol fuel cell, J. Electroanal. Chem. 654 (2011) 108–115.
[57] S. Mukerjee, J. McBreen, Effect of particle size on the electrocatalysis by carbon-supported Pt electrocatalysts: an in situ XAS investigation1, J. Electroanal. Chem. 448 (1998) 163–171.
[58] M. Yin, J. Xu, Q. Li, J.O. Jensen, Y. Huang, L.N. Cleemann, N.J. Bjerrum, W. Xing, Highly active and stable Pt electrocatalysts promoted by antimony-doped SnO2 supports for oxygen reduction reactions, Appl. Catal. B Environ. 144 (2014) 112–120.
[59] M.V. Hohmann, A. Wachau, A. Klein, In situ Hall effect and conductivity measurements of ITO thin films, Solid State Ionics 262 (2014) 636–639.
[60] V. Brinzari, B.K. Cho, M. Kamei, G. Korotcenkov, Photoemission surface characterization of (001) In2O3 thin film through the interactions with oxygen, water and carbon monoxide: comparison with (111) orientation, Appl. Surf. Sci. 324 (2015) 123–133.